Towards a Co-Design Framework for Future Mobility Systems

Gioele Zardini (Corresponding Author)
Stanford University, Aeronautics and Astronautics
496 Lomita Mall, Stanford, CA 94305-4035, USA
E-mail: gzardini@ethz.ch

Nicolas Lanzetti
Stanford University, Aeronautics and Astronautics
496 Lomita Mall, Stanford, CA 94305-4035, USA
E-mail: lnicolas@ethz.ch

Mauro Salazar, Ph.D.
Stanford University, Aeronautics and Astronautics
496 Lomita Mall, Stanford, CA 94305-4035, USA
E-mail: samauro@stanford.edu

Andrea Censi, Ph.D.
ETH Zurich, Institute for Dynamic Systems and Control
Sonneggstrasse 3, 8092 Zurich, ZH-Switzerland
E-mail: acensi@ethz.ch

Emilio Frazzoli, Ph.D.
ETH Zurich, Institute for Dynamic Systems and Control
Sonneggstrasse 3, 8092 Zurich, ZH-Switzerland
E-mail: emilio.frazzoli@idsc.mavt.ethz.ch

Marco Pavone, Ph.D.
Stanford University, Aeronautics and Astronautics
496 Lomita Mall, Stanford, CA 94305-4035, USA
E-mail: pavone@stanford.edu

Word Count: 7241 words + 1 table(s) × 250 = 7491 words

Submission Date: October 8, 2019

1 **1. Abstract**
2 The design of Autonomous Vehicles (AVs) and the design of AVs-enabled mobility systems are
3 closely coupled. Indeed, knowledge about the intended service of AVs would impact their design
4 and deployment process, whilst insights about their technological development could significantly
5 affect transportation management decisions. This calls for tools to study such a coupling and
6 co-design AVs and AVs-enabled mobility systems in terms of different objectives. In this paper,
7 we instantiate a framework to address such co-design problems. In particular, we leverage the
8 recently developed theory of co-design to frame and solve the problem of designing and deploying
9 an intermodal Autonomous Mobility-on-Demand system, whereby AVs service travel demands
10 jointly with public transit, in terms of fleet sizing, vehicle autonomy, and public transit service
11 frequency. Our framework is modular and compositional, allowing to describe the design problem
12 as the interconnection of its individual components and to tackle it from a system-level perspective.
13 Moreover, it only requires very general monotonicity assumptions and it naturally handles multiple
14 objectives, delivering the *rational* solutions on the Pareto front and thus enabling policy makers
15 to select a solution through "political" criteria. To showcase our methodology, we present a real-
16 world case study for Washington D.C., USA. Our work suggests that it is possible to create user-
17 friendly optimization tools to systematically assess the costs and benefits of interventions, and that
18 such analytical techniques might gain a momentous role in policy-making in the future.
19
20 *Keywords*: Co-Design, Autonomous Vehicles, Future Mobility Systems.

2. Introduction

Arguably, the current design process for Autonomous Vehicles (AVs) largely suffers from the lack of clear, specific requirements in terms of the service such vehicles will be providing. Yet, knowledge about their intended service (e.g., last-mile versus point-to-point travel) might dramatically impact how the AVs are designed, and, critically, significantly ease their development process. For example, if for a given city we knew that for an effective on-demand mobility system autonomous cars only need to drive up to 25 mph and only on relatively easy roads, their design would be greatly simplified and their deployment could certainly be accelerated. At the same time, from the system-level perspective of transportation management, knowledge about the trajectory of technology development for AVs would certainly impact decisions on infrastructure investments and provision of service. In other words, the design of the AVs and the design of a mobility system leveraging AVs are intimately *coupled*. This calls for methods to reason about such a coupling, and in particular to *co-design* the AVs and the associated AVs-enabled mobility system. A key requirement in this context is to be able to account for a range of heterogeneous objectives that are often not directly comparable (consider, for instance, travel time and emissions).

Accordingly, the goal of this paper is to lay the foundations for a framework through which one can co-design future AVs-enabled mobility systems. Specifically, we show how one can leverage the recently developed mathematical theory of co-design [1–3], which provides a general methodology to co-design complex systems in a modular and compositional fashion. This tool delivers the set of rational design solutions lying on the Pareto front, allowing to reason about the costs and benefits of the individual design options. The framework is instantiated in the setting of co-designing intermodal Autonomous Mobility-on-Demand (AMoD) systems [4], whereby fleets of self-driving vehicles provide on-demand mobility jointly with public transit. Aspects that are subject to co-design include fleet size, vehicle-specific characteristics for the AVs, and public transit service frequency.

Literature Review: The design of mobility systems can be divided in classic urban transportation network design problems and more recent design problems for AMoD systems. The first research stream was reviewed in [5] and can be divided in road [6, 7], public transit [8, 9], and multi-modal [10] network design problems which can be classified as *strategic* long-term infrastructure modification decisions such as building new streets, *tactical* infrastructure-allocation problems on lanes allocation and public transit service frequency, and *operational* short-term scheduling problems. They are usually formulated as bilevel problems whereby the upper-level is related to the policy in discussion and the lower-level is concerned with solving the trip assignment problem by computing the user equilibrium or the system optimum under given congestion and demand models. Overall, these problems are solved with non-convex and combinatorial mathematical methods, heuristics, and metaheuristics consisting of gradient-free optimization algorithms. Often, the problems are formulated with a unique objective or, in the case of multi-objective settings, the different objectives are reduced to a unique one through monetary metrics precluding Pareto solutions. The design of AMoD systems mostly considers their fleet sizing. In particular, it was studied through simulations in [11–13] and with analytical methods in [14], whilst in [15] the problem was combined with the charging infrastructure sizing and placement problem and solved using mixed integer linear programming techniques. The fleet sizing and vehicle allocation problem for conventional vehicles was presented in [16]. The fleet size and pricing scheme of Mobility-on-Demand systems was designed in [17] with Bayesian optimization, whereas in [18] a rail-car fleet sizing problem was solved with simulated annealing. More recently, the joint design of multimodal

1 transit networks and AMoD systems was formulated in [*19*] as a bilevel optimization problem and
2 solved with heuristic methods. Overall, to the best of the authors' knowledge, most design meth-
3 ods for AMoD rely either on simulation-based approaches or nonlinear and combinatorial opti-
4 mization techniques, and do not study AVs-specific characteristics such as the achievable vehicle
5 speed. In conclusion, the frameworks proposed for the design of mobility systems mainly have a
6 fixed problem-specific structure and are thus non-modular. Moreover, they do not deliver a Pareto
7 front of solutions, focusing on a unique objective.

8   *Statement of Contribution:* In this paper we lay the foundations for the systematic study of
9 the design of AVs-enabled mobility systems. Specifically, we leverage the mathematical theory of
10 co-design [*1*] to devise a framework to study the design of intermodal AMoD (I-AMoD) systems
11 in terms of fleet characteristics and public transit service, enabling the computation of the *ratio-*
12 *nal* solutions lying on the Pareto front of minimal travel time, transportation costs, and emissions.
13 Our framework allows to structure the design problem in a modular way, in which each different
14 transportation option can be "plugged in" in a larger model. Each model has minimal assump-
15 tions: Rather than properties such as linearity and convexity, we ask for very general monotonicity
16 assumptions. For example, we assume that the cost of automation increases monotonically with
17 the speed achievable by the self-driving car. We are able to obtain the full Pareto front of *rational*
18 solutions, or, given more "political" criteria, to weigh incomparable costs (such as travel time and
19 emissions), to present one optimal solution to stakeholders, such as AVs companies and municipal-
20 ities. We consider the real-world case study for Washington D.C., to showcase our methodology.
21 We show how, given the model, we can easily formulate and answer several questions regarding
22 the introduction of new technologies and investigate possible infrastructure interventions.

2.1. Organization

24 The remainder of this paper is structured as follows: Section 3 presents the mathematical back-
25 ground of co-design. Section 4 presents the co-design problem for AVs-enabled mobility systems.
26 We showcase our approach with real-world case studies for Washington D.C., USA, in Section 5.
27 Section 6 concludes the paper with a discussion and an overview on future research directions.

3. Mathematical Background

29 In this section, we present the basics of partial order theory and the mathematical theory of co-
30 design. The interested reader is referred to [*1–3*].

Partial Order Theory

32 Consider a set $\mathscr{P}$ and a partial order $\preceq_{\mathscr{P}}$, defined as a reflexive, antisymmetric, and transitive
33 relation [*20*]. Then, $\mathscr{P}$ and $\preceq_{\mathscr{P}}$ define the partially ordered set (poset) $\langle \mathscr{P}, \preceq_{\mathscr{P}} \rangle$. The least
34 and maximum elements of a poset are called bottom and top, and are denoted by $\bot_{\mathscr{P}}$ and $\top_{\mathscr{P}}$,
35 respectively. A set $S \subseteq \mathscr{P}$ is *directed* if each pair of elements $x, y \in S$ has an upper bound. A
36 poset is a *directed complete partial order* (DCPO) if each of its directed subsets has a top, and it
37 is a *complete partial order* (CPO) if it has a bottom as well. A *chain* is a subset $S \subseteq \mathscr{P}$ where
38 all elements are comparable, i.e., for $x, y \in S$, $x \preceq_{\mathscr{P}} y$ or $y \preceq_{\mathscr{P}} x$. Conversely, an *antichain* is a
39 subset $S \subseteq \mathscr{P}$ where no elements are comparable, i.e., for $x, y \in S$, $x \preceq_{\mathscr{P}} y$ implies $x = y$. A map
40 $g : \mathscr{P} \to \mathscr{Q}$ between two posets is *monotone* iff $x \preceq_{\mathscr{P}} y$ implies $g(x) \preceq_{\mathscr{Q}} g(y)$.

Mathematical Theory of Co-Design

42 As in [*1*], we abstract a Design Problem (DP) as a monotone map h between provided *function-*

1 *alities* and the antichain of required *resources*, represented as elements of the CPOs $\langle \mathscr{F}, \preceq_{\mathscr{F}} \rangle$,
2 $\langle \mathscr{R}, \preceq_{\mathscr{R}} \rangle$, respectively. Different to classical approaches, mostly relying on properties such as
3 continuity, linearity, or convexity, our approach only requires monotone relations between the an-
4 tichain of resources and the functionalities. The Co-Design Problem (CDP) of the full system
5 results then from the interconnection, typically given in form of a graph, of the DP of its individ-
6 ual components. Indeed, this allows to describe complex models in a modular and compositional
7 fashion. We focus on the problem of finding the antichain of all *rational* resources $r_1, \ldots, r_N \in \mathscr{R}$
8 which provide a given functionality $f \in \mathscr{F}$. Nevertheless, the framework can readily accommo-
9 date alternative problem formulations, such as finding the antichain of all rational functionalities
10 $f_1, \ldots, f_N \in \mathscr{F}$ which are provided given a resource $r \in \mathscr{R}$. Rather than computing a single solu-
11 tion, this method provides therefore an antichain, or equivalently, a set of incomparable rational
12 decisions.

13 4. Co-Design of AV-enabled Mobility Systems

14 In this section, we instantiate our proposed co-desing framework in the setting whereby a central,
15 social welfare maximizing authority (e.g., a central authority) strives to co-design a mobility sys-
16 tem comprising AMoD and public transportation, in terms of AV fleet size, vehicle-specific char-
17 acteristics, and public transit service frequency. This rather idealized setting serves a number of
18 purposes: First, it grounds our co-design framework within a concrete urban transportation design
19 problem. Second, the insights we derive can be interpreted as upper bounds on the performance
20 gains one might achieve via co-design. Third, this setting subsumes as special cases the co-design
21 of AV and AMoD services (of interest, e.g., to AV and mobility-as-a-service companies alike) and
22 the co-design of AMoD and intermodal transportation systems (of interest, e.g., to municipal au-
23 thorities). Fourth, it provides a starting point to address the more challenging (and more realistic)
24 setting whereby multiple stakeholders, with different objectives, might converge via co-design to
25 an optimized transportation system.
26 We start by describing in Section 4.1 the urban transportation design problem we want to
27 address in this paper; we then present its associated co-desing framework in Section 4.2.

28 4.1. Intermodal AMoD Framework

29 In this section, we present the I-AMoD framework from [*4*] used to describe our setting. We adopt
30 a mesoscopic planning perspective and formulate the problem as a multi-commodity network flow
31 problem, whereby we allow customers to be routed in an intermodal fashion.

32 *4.1.1. Multi-Commodity Flow Model*

33 The transportation system and its different modes are modeled using the digraph $\mathscr{G} = (\mathscr{V}, \mathscr{A})$,
34 shown in Figure 1a. It is composed of a set of nodes $\mathscr{V}$ and a set of arcs $\mathscr{A} \subseteq \mathscr{V} \times \mathscr{V}$. Specifically,
35 it contains a road network layer $\mathscr{G}_R = (\mathscr{V}_R, \mathscr{A}_R)$, a public transportation layer $\mathscr{G}_P = (\mathscr{V}_P, \mathscr{A}_P)$, and a
36 walking layer $\mathscr{G}_W = (\mathscr{V}_W, \mathscr{A}_W)$. The road network is characterized through intersections $i \in \mathscr{V}_R$ and
37 road segments $(i, j) \in \mathscr{A}_R$. Similarly, public transportation lines are modeled through station nodes
38 $i \in \mathscr{V}_P$ and line segments $(i, j) \in \mathscr{A}_P$. The walking network contains walkable streets $(i, j) \in \mathscr{A}_W$
39 connecting intersections $i \in \mathscr{V}_W$. Our model allows mode-switching arcs $\mathscr{A}_C \subseteq \mathscr{V}_R \times \mathscr{V}_W \cup \mathscr{V}_W \times$
40 $\mathscr{V}_R \cup \mathscr{V}_P \times \mathscr{V}_W \cup \mathscr{V}_W \times \mathscr{V}_P$ connecting the road and the public transportation layers to the pedestrian
41 layer. Consequently, $\mathscr{V} = \mathscr{V}_W \cup \mathscr{V}_R \cup \mathscr{V}_P$ and $\mathscr{A} = \mathscr{A}_W \cup \mathscr{A}_R \cup \mathscr{A}_P \cup \mathscr{A}_C$. Consistently with the
42 structural properties of road and walking networks in urban environments, we assume the graph $\mathscr{G}$
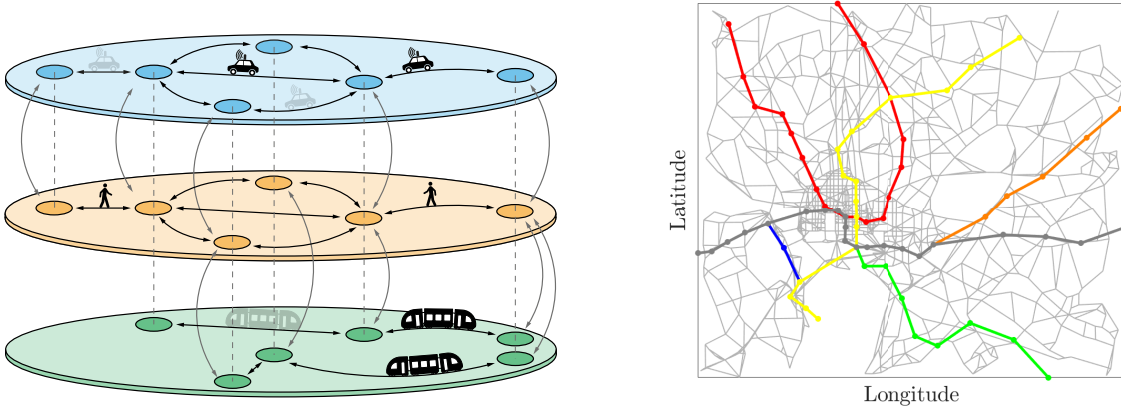
(a) Intermodal AMoD network.

(b) Washington D.C. road and subway graphs.

FIGURE 1: (a) The intermodal AMoD network consists of a road, a walking, and a public transportation digraph. The coloured circles represent stops or intersections and the black arrows denote road links, pedestrian pathways, or public transit arcs. The dotted lines represent nodes which are close geographically, while the grey arrows represent the mode-switching arcs connecting them. (b) The Washington D.C. transportation network, consisting of the MetroRail subway lines and the city roads.

1   to be strongly connected. We model a travel request ρ as a triple $(o, d, \alpha) \in \mathscr{V} \times \mathscr{V} \times \mathbb{R}_+$, described
2   by its origin node o, its destination node d, and its request rate $\alpha > 0$, namely, how many customers
3   want to travel from o to d per unit time. We assume that the origin and destination vertices of the
4   M requests lie in the walking digraph, i.e., $o_m, d_m \in \mathscr{V}_W$ for all $m \in \mathscr{M} := \{1, \ldots, M\}$.
5   The flow $f_m(i, j)$ represents the number of customers per unit time traversing arc $(i, j) \in \mathscr{A}$
6   and satisfying a travel request m. Furthermore, $f_0(i, j)$ denotes the flow of empty vehicles on road
7   arcs $(i, j) \in \mathscr{A}_R$, accounting for rebalancing flows of AMoD vehicles between a customer's drop-
8   off and the next customer's pick-up. Assuming the vehicles to carry one customer at a time, the
9   flows satisfy

10
$$\sum_{i:(i,j)\in\mathscr{A}} f_m(i,j) + \mathbb{1}_{j=o_m} \cdot \alpha_m = \sum_{k:(j,k)\in\mathscr{A}} f_m(j,k) + \mathbb{1}_{j=d_m} \cdot \alpha_m, \quad \forall m \in \mathscr{M}, j \in \mathscr{V} \tag{1a}$$

11
$$\sum_{i:(i,j)\in\mathscr{A}_R} \left(f_0(i,j) + \sum_{m\in\mathscr{M}} f_m(i,j) \right) = \sum_{k:(j,k)\in\mathscr{A}_R} \left(f_0(j,k) + \sum_{m\in\mathscr{M}} f_m(j,k) \right), \quad \forall j \in \mathscr{V}_R \tag{1b}$$

12
$$f_m(i,j) \geq 0, \quad \forall m \in \mathscr{M}, (i,j) \in \mathscr{A} \tag{1c}$$

13
14
$$f_0(i,j) \geq 0, \quad \forall (i,j) \in \mathscr{A}_R, \tag{1d}$$

15   where $\mathbb{1}_{j=x}$ denotes the boolean indicator function. Specifically, (1a) guarantees flows conservation
16   for every transportation demand, and (1b) preserves flow conservation for vehicles on every road
17   node. Combining conservation of customers (1a) with the conservation of vehicles (1b) guarantees
18   rebalancing vehicles to match the demand. Finally, (1c), (1d) ensure non-negativity of flows.

1 *4.1.2. Travel Time and Travel Speed*
2 The variable t_{ij} denotes the time needed to traverse an arc (i, j) of length s_{ij}. We assume a constant
3 walking speed on pedestrian arcs and infer travel times on public transportation arcs from the
4 public transit schedules. Considering that the public transportation system at node j operates with
5 the frequency φ_j, switching from a pedestrian vertex i to a public transit station j takes, on average,
6 $t_{\mathrm{WS}} + 1/\varphi_j$, where t_{WS} is a constant sidewalk-to-station travel time. We assume that the average
7 waiting time for AMoD vehicles is t_{WR} and that switching from the road graph and the public
8 transit graph to the pedestrian graph takes the transfer times t_{RW} and t_{SW}, respectively. While each
9 road arc $(i, j) \in \mathscr{A}_{\mathrm{R}}$ is characterized by a speed limit $v_{\mathrm{L},ij}$, AVs safety protocols impose a maximum
10 achievable velocity v_{a}. In order to prevent too slow and therefore dangerous driving behaviours
11 [21], we only consider road arcs through which the AVs can drive at least at a fraction β of the
12 speed limit: Arc $(i, j) \in \mathscr{A}_{\mathrm{R}}$ is kept in the road network if and only if

13
$$v_{\mathrm{a}} \geq \beta \cdot v_{\mathrm{L},ij}, \tag{2}$$

14 where $\beta \in (0, 1]$. We set the velocity of all arcs fulfilling condition (2) to $v_{ij} = \min\{v_{\mathrm{a}}, v_{\mathrm{L},ij}\}$ and
15 compute the travel time to traverse them as

16
$$t_{ij} = \frac{s_{ij}}{v_{ij}}. \tag{3}$$

17 *4.1.3. Road Congestion*
18 In our setting, we assume that each road arc $(i, j) \in \mathscr{A}_{\mathrm{R}}$ is subject to a baseline usage u_{ij}, capturing
19 the presence of exogenous traffic (e.g., private vehicles), and that it has a nominal capacity c_{ij}.
20 Furthermore, we assume that the central authority operates the AMoD fleet such that vehicles
21 travel at free-flow speed throughout the road network of the city, meaning that the total flow on
22 each road link must be below the link's capacity. Therefore, we capture congestion effects with the
23 threshold model

24
$$f_0(i, j) + \sum_{m \in \mathscr{M}} f_m(i, j) + u_{ij} \leq c_{ij} \quad \forall (i, j) \in \mathscr{A}_{\mathrm{R}}. \tag{4}$$

25 *4.1.4. Energy Consumption*
26 We compute the energy consumption of the AVs for each road link considering an urban driving
27 cycle, scaled so that the average speed $v_{\mathrm{avg,cycle}}$ matches the free-flow speed on the link s_{ij}/t_{ij}, and
28 scale the energy consumption with the length of the arc s_{ij} as

29
$$e_{ij} = e_{\mathrm{cycle}} \cdot \frac{s_{ij}}{s_{\mathrm{cycle}}} \quad \forall (i, j) \in \mathscr{A}_{\mathrm{R}}. \tag{5}$$

30 For the public transportation system, we assume a constant energy consumption per unit time. This
31 approximation is acceptable in urban environments, as the operation of the public transportation
32 system is independent from the number of customers serviced, and its energy consumption is
33 therefore customers-invariant.

34 *4.1.5. Fleet Size*
35 We consider a fleet of $n_{\mathrm{v,max}}$ AVs. In a time-invariant setting, the number of vehicles on arc (i, j) is
36 expressed as the multiplication of the total vehicles flow on the arc and its travel time. Therefore,

we constrain the number of vehicles employed as

$$n_{v,e} = \sum_{(i,j) \in \mathscr{A}_R} \left(f_0(i,j) + \sum_{m \in \mathscr{M}} f_m(i,j) \right) \cdot t_{ij} \leq n_{v,max}. \tag{6}$$

4.1.6. Discussion

A few comments are in order. First, we assume the demand to be time-invariant and allow flows to have fractional values. This assumption is in line with the *mesoscopic* and system-level *planning* perspective of our study. Second, we model congestion using a threshold model. This approach can be interpreted as the municipal authority not allowing the AMoD vehicles to exceed the critical density of the flows on road arcs, so that cars can be assumed to travel at free flow speed [22]. This way, we can assume that the route planning of AMoD vehicles does not influence the exogenous traffic. Finally, in line with the status quo, we allow AMoD vehicles to transport one customer at the time [23]. For further discussions on our modeling assumptions, we refer the readers to [4, 24].

4.2. Co-Design Framework

We integrate the I-AMoD framework presented in Section 4.1 in the co-design formalism, allowing the decoupling of the CDP of a complex system in the DP of its individual components in a modular, compositional, and systematic fashion. We aim to compute the antichain of resources, quantified in terms of costs, average travel time per trip, and emissions required to provide the mobility service to a set of customers. In order to achieve this, we decouple the CDP in the DPs of the individual AV (Section 4.2.1) and of the AVs fleet (Section 4.2.3) as well as of the public transportation system (Section 4.2.2). Their interconnection is presented in Section 4.2.4.

4.2.1. The Autonomous Vehicle Design Problem

The AV DP (Figure 2a) consists of selecting the maximal speed of the AVs. Under the rationale that driving safely at higher speed requires more advanced sensing and algorithmic capabilities, we model the achievable speed of the AVs v_a as a monotone function of the vehicle fixed costs $C_{v,f}$ (resulting from the cost of the vehicle $C_{v,v}$ and the cost of its automation $C_{v,a}$) and the mileage-dependent operational costs $C_{v,o}$ (accounting for maintenance, cleaning, energy consumption, depreciation, and opportunity costs [25]). In this setting, the AV DP provides the functionality v_a and requires the resources $C_{v,f}$ and $C_{v,o}$. Consequently, the functionality space is $\mathscr{F}_v = \overline{\mathbb{R}}_+$ (in mph), and the resources space is $\mathscr{R}_v = \overline{\mathbb{R}}_+ \times \overline{\mathbb{R}}_+$ (in USD $\times$ USD/mile).

4.2.2. The Subway Design Problem

We design the public transit infrastructure (Figure 2b) by means of the service frequency introduced in Section 4.1.2. Specifically, we assume the service frequency φ_j to scale linearly with the size of the train fleet n_s as

$$\frac{\varphi_j}{\varphi_{j,baseline}} = \frac{n_s}{n_{s,baseline}}. \tag{7}$$

We relate a train fleet of size n_s to the fixed costs $C_{s,f}$ (accounting for train and infrastructural costs) and to the operational costs $C_{s,o}$ (accounting for energy consumption, vehicles depreciation, and train operators' wages). Given the passengers-independent public transit operation in today's cities, we reasonably assume the operational costs $C_{s,o}$ to be mileage independent and to only

1   vary with the size of the fleet. Formally, the number of acquired trains $n_{s,a} = n_s - n_{s,baseline}$ is
2   a functionality, whereas $C_{s,f}$ and $C_{s,o}$ are resources. The functionality space is $\mathscr{F}_s = \mathbb{N}$ and the
3   resources space is $\mathscr{R}_s = \overline{\mathbb{R}}_+ \times \overline{\mathbb{R}}_+$ (in USD $\times$ USD/year).

4   *4.2.3. The I-AMoD Optimization Framework Design Problem*
5   The I-AMoD DP (see Figure 2c) provides the demand satisfaction as a functionality, expressed
6   through the total customer request rate

7   $$\alpha_{tot} := \sum_{m \in \mathscr{M}} \alpha_m. \tag{8}$$

8   To successfully satisfy a given set of travel requests, we require the following resources: (i) the
9   achievable speed of the AVs v_a, (ii) the number of available AVs per fleet $n_{v,max}$, (iii) the number
10 of trains $n_{s,a}$ acquired by the public transportation system, and (iv) the average travel time of a trip

11 $$t_{avg} := \frac{1}{\alpha_{tot}} \cdot \sum_{m \in \mathscr{M}, (i,j) \in \mathscr{A}} t_{ij} \cdot f_m(i,j), \tag{9}$$

12 (v) the total distance driven by the AVs per unit time

13 $$s_{v,tot} := \sum_{(i,j) \in \mathscr{A}_R} s_{ij} \cdot \left(f_0(i,j) + \sum_{m \in \mathscr{M}} f_m(i,j) \right), \tag{10}$$

14 and (vi) the total AVs CO_2 emissions per unit time

15 $$m_{CO_2,v,tot} := \gamma \cdot \sum_{(i,j) \in \mathscr{A}_R} e_{ij} \cdot \left(f_0(i,j) + \sum_{m \in \mathscr{M}} f_m(i,j) \right), \tag{11}$$

16 where γ relates the energy consumption and the CO_2 emissions. We assume that customers trips
17 and AMoD rebalancing strategies are chosen to maximize the customers welfare, defined through
18 the average travel time t_{avg}. Hence, we link the functionality and resources of the I-AMoD DP
19 through the following optimization problem:

20 $$\min_{\{f_m(\cdot,\cdot)\}_m, f_0(\cdot,\cdot)} t_{avg} = \frac{1}{\alpha_{tot}} \sum_{m \in \mathscr{M}, (i,j) \in \mathscr{A}} t_{ij} \cdot f_m(i,j) \quad \text{s.t. Eq. (1), Eq. (4), Eq. (6).} \tag{12}$$

21 Formally, $\mathscr{F}_o = \overline{\mathbb{R}}_+$, and $\mathscr{R}_o = \overline{\mathbb{R}}_+ \times \overline{\mathbb{N}} \times \overline{\mathbb{N}} \times \overline{\mathbb{R}}_+ \times \overline{\mathbb{R}}_+ \times \overline{\mathbb{R}}_+$. Note that in general, the optimization
22 problem (12) might possess multiple optimal solutions, making the relation between resources and
23 functionality ill-posed. To overcome this subtlety, if two solutions share the same average travel
24 time, we select the one incurring in the *lowest* mileage.

25 *4.2.4. The Monotone Co-Design Problem*
26 The full-system CDP results from the interconnection of the DPs presented above. A schematic
27 representation is shown in Figure 2d. The functionality of the system is to provide mobility service
28 to the customers, quantified, as in (8), by means of the total request rate. To this end, the following
29 three resources are required. First, on the customers side, we require an average travel time, defined
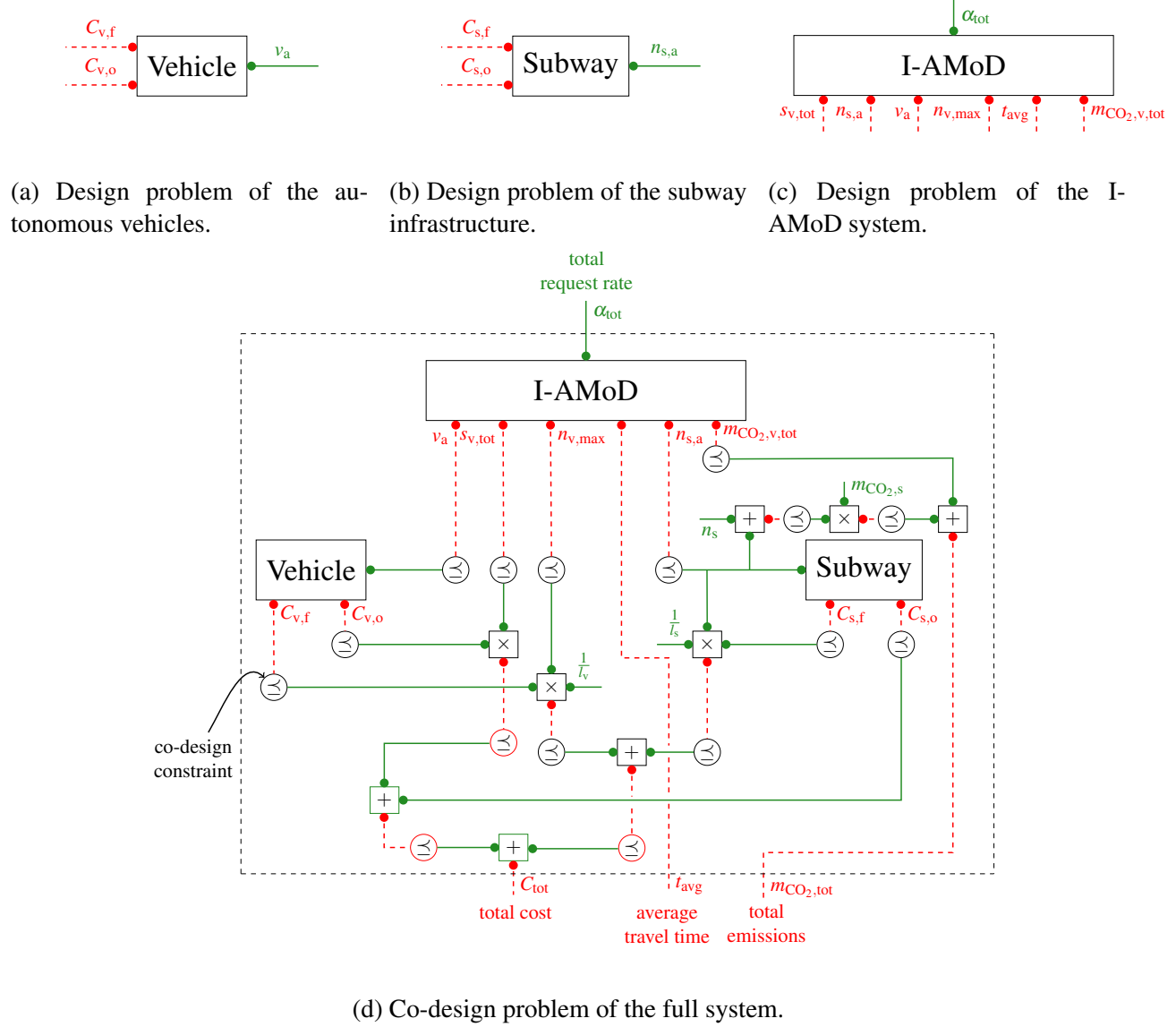
(a) Design problem of the autonomous vehicles.

(b) Design problem of the subway infrastructure.

(c) Design problem of the I-AMoD system.

(d) Co-design problem of the full system.

FIGURE 2: Schematic representation of the individual design problems (a-c) as well as of the co-design problem of the full system (d). In solid green the provided functionalities and in dashed red the required resources. The edges in the co-design diagram (d) represent co-design constraints: The resources required by a first design problem are the lower bound for the functionalities provided by the second one.

as in (9). Second, on the central authority side, the resource is the total transportation cost of the intermodal mobility system: Assuming an average vehicles' life of l_v, an average trains' life of l_s, and a baseline subway fleet of $n_{s,baseline}$ trains, we express the total costs as

$$C_{tot} = C_v + C_s, \tag{13}$$

1   where C_v is the AVs-related cost

2   $$C_v = \frac{C_{v,f}}{l_v} \cdot n_v + C_{v,o} \cdot s_{v,tot},$$ (14)

3   and C_s is the public transit-related cost

4   $$C_s = \frac{C_{s,f}}{l_s} \cdot n_{s,a} + C_{s,o}.$$ (15)

5   Third, on the environmental side, the resources is the total CO_2 emissions

6   $$m_{CO_2,tot} = m_{CO_2,v,tot} + m_{CO_2,s} \cdot n_s,$$ (16)

7   where $m_{CO_2,s}$ represents the CO_2 emissions of a single train. Formally, α_{tot} is the CDP function-
8   ality, whereas t_{avg}, C_{tot}, and $m_{CO_2,tot}$ are the resources. Consistently, the functionality space is
9   $\mathscr{F} = \overline{\mathbb{R}}_+$ and the resources space is $\mathscr{R} = \overline{\mathbb{R}}_+ \times \overline{\mathbb{R}}_+ \times \overline{\mathbb{R}}_+$. Note that the resulting CDP is indeed
10 monotone, since it consists of the interconnection of monotone DPs [1].

11 **4.3. Discussion**
12 A few comments are in order. First, we lump the vehicle autonomy in its achievable velocity.
13 We leave to future research more elaborated AV models, accounting for instance for accidents
14 rates [26] and for safety levels. Second, we assume the service frequency of the subway system
15 to scale linearly with the number of trains. We inherently rely on the assumption that the existing
16 infrastructure can homogeneously accommodate the acquired train cars. To justify the assumption,
17 we include an upper bound on the number of potentially acquirable trains in our case study design
18 in Section 5. Third, we highlight that the I-AMoD framework is only one of the many feasible
19 ways to map total demand to travel time, costs, and emissions. Specifically, practitioners can easily
20 replace the corresponding DP with more sophisticated models (e.g., simulation-based frameworks
21 like MATSim [27]), as long as the monotonicity of the system is preserved. In our setting, we
22 conjecture the customers and vehicles routes to be centrally controlled by the central authority in a
23 socially-optimal fashion. Fourth, we assume a homogenous fleet of AVs. Nevertheless, our model
24 is readily extendable to capture heterogeneous fleets. Finally, we consider a fixed travel demand,
25 and compute the antichain of resources providing it. Nonetheless, our formalization can be readily
26 extended to arbitrary demand models preserving the monotonicity of the CDP (accounting for
27 instance for elastic and stochastic effects). We leave this topic to future research.

28 **5. Results**
29 In this section, we leverage the framework presented in Section 4 to evaluate the real-world case
30 of Washington D.C., USA. Section 5.1 details the case study. We then present numerical results in
31 Sections 5.2 and 5.3.

32 **5.1. Case Study**
33 We present our studies on the real-world case of Washington D.C., USA. We import the road net-
34 work (Figure 1b) and its features from OpenStreetMap [28]. The public transit network and its
35 schedules are extracted from the GTFS data [29]. The travel demand is obtained by unifying the
36 origin-destination pairs of the morning peak of May 31st 2017 provided by the taxi companies [30]

1 and the Washington Metropolitan Area Transit Authority (WMATA) [23]. Given the lack of re-
2 liable demand data for the MetroBus system, we focus our studies on the MetroRail system and
3 its design, inherently assuming MetroBus commuters to be unaffected by our design methodology.
4 To account for the large presence of ride-hailing companies, we scale the taxi demand rate by a
5 factor of 5 [31]. Overall, the demand dataset includes 15,872 travel requests, corresponding to a
6 demand rate of 24.22 requests/s. To account for congestion effects, we compute the nominal road
7 capacity as in [32] and assume an average baseline road usage of 93%, in line with [33]. We sum-
8 marize the main parameters together with their bibliographic sources in Table 1. In the remainder
9 of this section, we tailor and solve the co-design problem presented in Section 4 through the PyM-
10 CDP solver [34], and investigate the influence of different AVs costs on the design objectives and
11 strategies.

Parameter		Variable		Value				Units	Source
Baseline road usage		u_{ij}		93				%	[33]
			Case 1	Case 2.1	Case 2.2	Case 3.1	Case 3.2		
Vehicle operational cost		$C_{v,o}$	0.084	0.084	0.062	0.084	0.084	USD/mile	[35, 36]
Vehicle cost		$C_{v,v}$	32,000	32,000	26,000	32,000	32,000	USD/car	[35]
	20 mph		15,000	20,000	3,700	0	500,000	USD/car	[36–40]
	25 mph		15,000	30,000	4,400	0	500,000	USD/car	[36–40]
	30 mph		15,000	55,000	6,200	0	500,000	USD/car	[36–40]
Vehicle automation cost	35 mph	$C_{v,a}$	15,000	90,000	8,700	0	500,000	USD/car	[36–40]
	40 mph		15,000	115,000	9,800	0	500,000	USD/car	[36–40]
	45 mph		15,000	130,000	12,000	0	500,000	USD/car	[36–40]
	50 mph		15,000	150,000	13,000	0	500,000	USD/car	[36–40]
Vehicle life		l_v	5	5	5	5	5	years	[35]
CO_2 per Joule		γ	0.14	0.14	0.14	0.14	0.14	g/kJ	[41]
Time from $\mathscr{G}_W$ to $\mathscr{G}_R$		t_{WR}	300	300	300	300	300	s	-
Time from $\mathscr{G}_R$ to $\mathscr{G}_W$		t_{RW}	60	60	60	60	60	s	-
Speed limit fraction		β	$\frac{1}{1.3}$	$\frac{1}{1.3}$	$\frac{1}{1.3}$	$\frac{1}{1.3}$	$\frac{1}{1.3}$	-	[21]
	100 %				148,000,000			USD/year	[42]
Subway operational cost	133 %	$C_{s,o}$			197,000,000			USD/year	[42]
	200 %				295,000,000			USD/year	[42]
Subway fixed cost		$C_{s,f}$			14,500,000			USD/train	[43]
Train life		l_s			30			years	[43]
Subway CO_2 emissions per train		$m_{CO_2,s}$			140			ton/year	[44]
Train fleet baseline		$n_{s,baseline}$			112			trains	[43]
Subway service frequency		$\varphi_{j,baseline}$			$\frac{1}{6}$			1/minutes	[45]
Time from $\mathscr{G}_W$ to $\mathscr{G}_P$ and vice-versa		t_{WS}			60			s	-

**TABLE 1**: Parameters, variables, numbers, and units for the case studies.

12 **5.2. Case 1 - Constant Cost of Automation**
13 In line with [36–40], we first assume an average achievable-velocity-independent cost of automa-
14 tion. As discussed in Section 4, we design the system by means of subway service frequency, AVs
15 fleet size, and achievable free-flow speed. Specifically, we allow the municipality to (i) increase
16 the subway service frequency φ_j by a factor of 0%, 33%, or 100%, (ii) deploy an AMoD fleet of
17 size $n_{v,max} \in \{0, 500, 1000, \ldots, 6000\}$ vehicles, and (iii) design the single AV achievable velocity
18 $v_a \in \{20\,\text{mph}, 25\,\text{mph}, \ldots, 50\,\text{mph}\}$. We assume the AMoD fleet to be composed of battery elec-
19 tric BEV-250 mile vehicles [35]. In Figure 3a, we show the solution of the co-design problem
20 by reporting the antichain consisting of the total transportation cost, average travel time, and total
21 CO_2 emissions. These solutions are *rational* (and not comparable) in the sense that there exists

no instance which simultaneously yields lower cost, average travel time, and emissions. For the
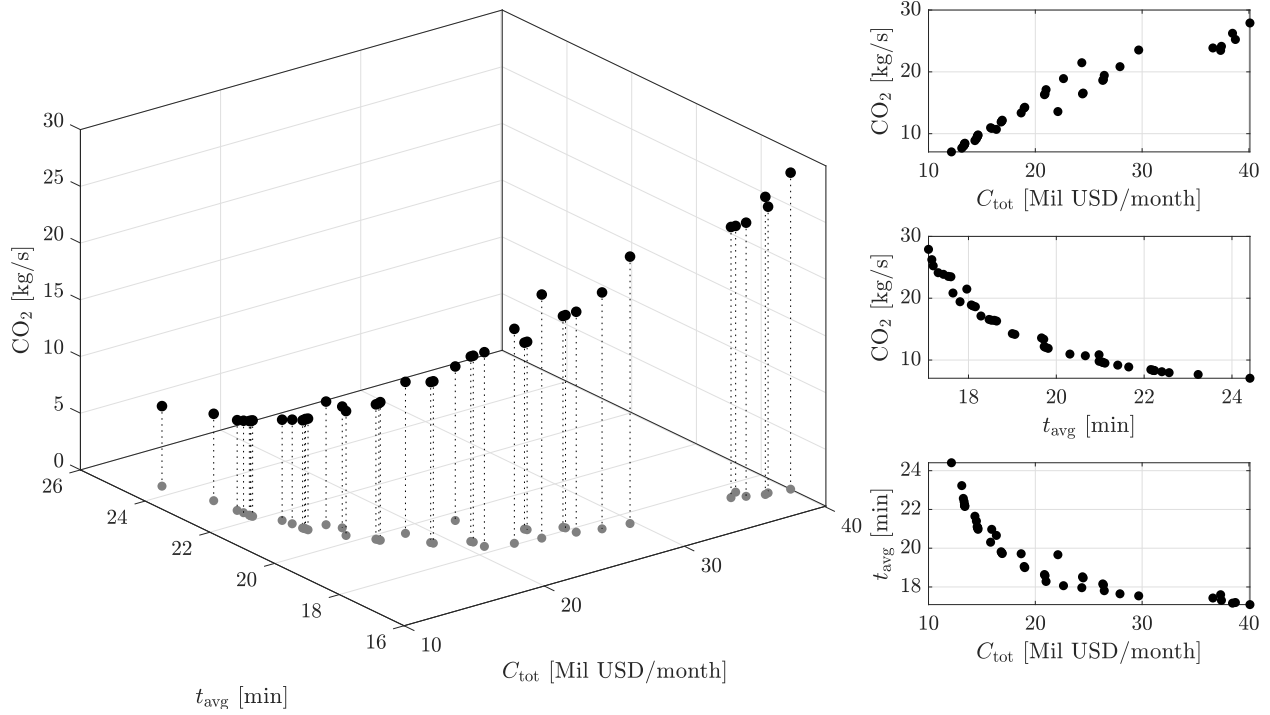
(a) Tri-dimensional representation antichain elements and their projection in the cost-time space (left) and their two-dimensional projections (right).
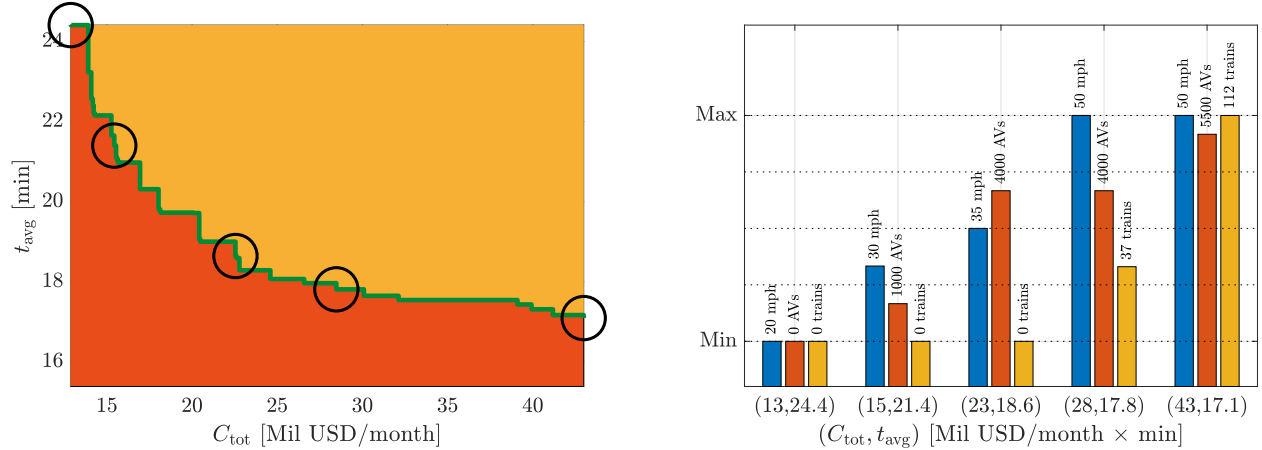
(b) Results for asymptotic automation costs. On the left, the two-dimensional representation of the antichain elements: in red are the unfeasible strategies, in orange the feasible but irrational solutions, and in green the Pareto front. On the right, the implementations corresponding to the highlighted antichain elements, quantified in terms of achievable vehicle speed, AVs fleet size, and train fleet size.

FIGURE 3: Solution of the Co-Design Problem (CDP) for the state-of-the art case.

1
2 sake of clarity, we opt for a two-dimensional antichain representation, by translating and includ-

1 ing the emissions in the total cost. To do so, we consider the conversion factor 40 $^{\mathrm{USD}}/\mathrm{kg}$ [46].
2 Note that since this transformation preserves the monotonicity of the CDP it smoothly integrates
3 in our framework. Doing so, we can conveniently depict the co-design strategies through the two-
4 dimensional antichain (Figure 3b, right) and the corresponding municipality actions (Figure 3b,
5 left). Generally, as the municipality budget increases, the average travel time per trip required to
6 satisfy the given demand decreases, reaching a minimum of about 17.1 minutes with a monthly
7 expense of around 43,000,000 $^{\mathrm{USD}}/\mathrm{month}$. This configuration corresponds to a fleet 5,500 AVs able
8 to drive at 50 mph and to the doubling of the current MetroRail train fleet. On the other hand,
9 the smallest rational investment of 12,900,000 $^{\mathrm{USD}}/\mathrm{month}$ leads to a 42 % higher average travel time,
10 corresponding to a non-existent autonomous fleet and an unchanged subway infrastructure. No-
11 tably, an expense of 23,000,000 $^{\mathrm{USD}}/\mathrm{month}$ (48 % lower than the highest rational investment) only
12 increases the minimal required travel time by 9 %, requiring a fleet of 4,000 vehicles able to drive
13 at 35 mph and no acquisition of trains. Conversely, an investment of 15,600,000 $^{\mathrm{USD}}/\mathrm{month}$ (just
14 2,700,000 $^{\mathrm{USD}}/\mathrm{month}$ more than the minimal rational investment) provides a 3 min shorter travel
15 time. Remarkably, the design of AVs able to exceed 40 mph only improves the average travel time
16 by 6 %, and it is rational just starting from an expense of 22,800,000 $^{\mathrm{USD}}/\mathrm{month}$. This suggests that
17 the design of faster vehicles mainly results in higher emission rates and costs, without substantially
18 contributing to a more time-efficient demand satisfaction. Finally, it is rational to improve the sub-
19 way system only starting from a budget 28,500,000 $^{\mathrm{USD}}/\mathrm{month}$, leading to a travel time improvement
20 of just 4 %. This trend can be explained with the high train acquisition and increased operation
21 costs, related to the subway reinforcement. We expect this phenomenon to be more marked for
22 other cities, considering the moderate operation costs of the MetroRail subway system due to its
23 automation [45] and related benefits [47].

5.3. Case 2 - Speed-Dependent Automation Costs

25 To relax the potentially unrealistic assumption of a velocity-independent automation cost, we con-
26 sider a performance-dependent cost structure. The large variance in sensing technologies and their
27 reported performances [48] suggests that this rationale is reasonable. Indeed, the technology re-
28 quired today to safely operate an autonomous vehicle at 50 mph is substantially more sophisticated,
29 and therefore more expensive, than the one needed at 20 mph. To this end, we adopt the cost struc-
30 ture reported in Table 1. Furthermore, the frenetic evolution of automation techniques intricates
31 their monetary quantification [49]. Therefore, we perform our studies with current (2019) costs as
32 well as with their projections for the upcoming decade (2025) [35, 50].

5.3.1. Case 2.1 - 2019

34 Here, we study the hypothetical case of an immediate AVs fleet deployment, assuming the techno-
35 logical advances to be provided. We introduce the aforementioned velocity-dependent automation
36 cost structure and obtain the results reported in Figure 4a. Comparing these results with the state-
37 of-the-art values presented in Figure 3 confirms the previously observed trend concerning elevated
38 vehicle speeds. Indeed, spending 24,900,000 $^{\mathrm{USD}}/\mathrm{month}$ (55 % lower than the highest rational ex-
39 pense) only increases the average travel time by 10 %, requiring a fleet of 3,000 AVs at 40 mph and
40 no subway interventions. Nevertheless, the comparison shows two substantial differences. First,
41 the budget required to reach the minimum travel time of 17.1 minutes is 28 % higher compared to
42 the previous case, and consists of the same strategy for the municipality, i.e., doubling the train
43 fleet and having a fleet of 5,500 AVs at 50 mph. Second, the higher vehicle costs result in an av-

1 erage AVs fleet growth of 5 %, an average velocity reduction of 9 %, and an average train fleet
2 growth of 7 %. The latter suggests a shift towards a poorer AVs performance in favour of fleets
enlargements.
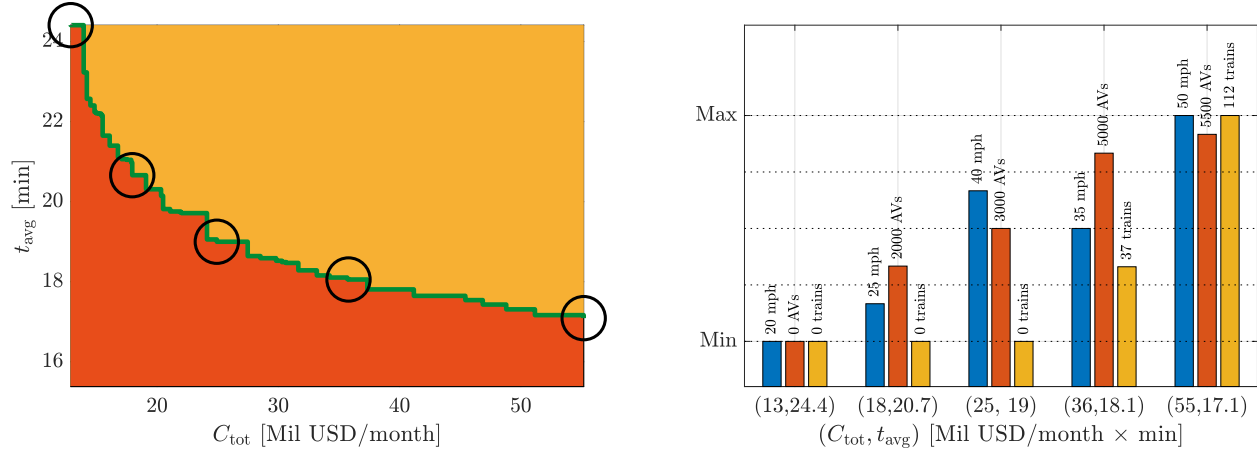
(a) Speed-dependent automation costs in 2019.
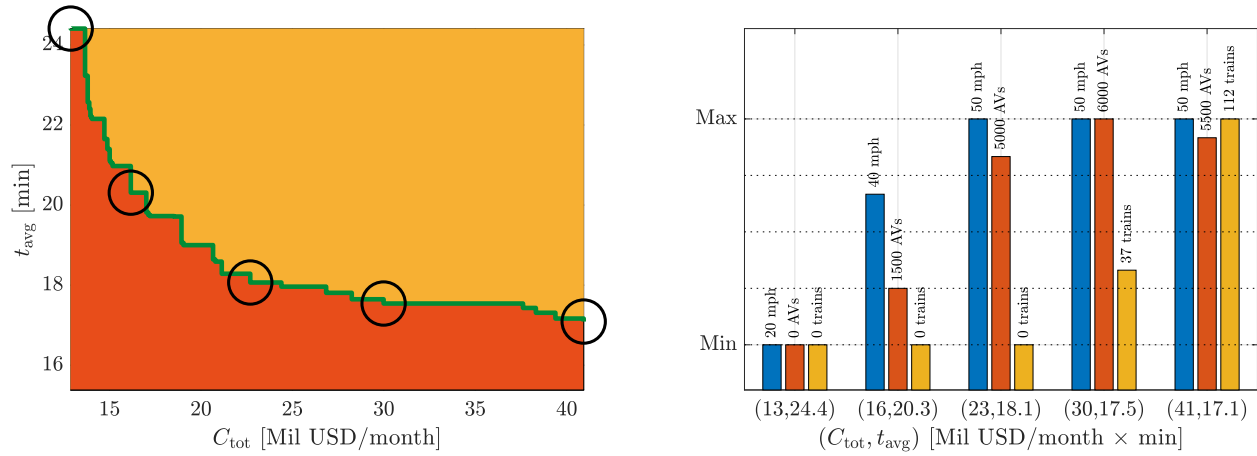
(b) Speed-dependent automation costs in 2025.

FIGURE 4: Results for the speed-dependent automation costs. On the left, the two-dimensional representation of the antichain elements: in red are the unfeasible strategies, in orange the feasible but irrational solutions, and in green the Pareto front. On the right, the implementations corresponding to the highlighted antichain elements.

3

4 *5.3.2. Case 2.2 - 2025*
5 Experts forecast a large automation cost reduction (up to 90 %) in the next decade, due to mass-
6 production of the AVs sensing technology [*49, 50*]. In line with this vision, we inspect the futuristic
7 scenario by solving the co-design problem for the adapted automation costs, and report the results
8 in Figure 4b. Two comments are in order. First, one can notice that the maximal rational budget is
9 25 % lower than in the immediate adoption case. Second, the reduction in autonomy costs clearly
10 eases the acquisition of more performant AVs, increasing the average vehicle speed by 10 %. As a
11 direct consequence, the AVs and train fleets are reduced in size by 5 % and 10 %, respectively.

5.4. Case 3 - Asymptotic Automation Cost Analysis

We conclude our numerical analysis with a study on asymptotic cost structures. Specifically, we compare the constrasting cases of a free-of-charge and a very high (500,000 USD/car) automation cost.

5.4.1. Case 3.1- No Automation Cost

This case could represent the future full deployment of AVs, where the cost of automation is naturally included in the normal production costs and does not represent an additional expense. The results for this cost structure are reported in Figure 5a. Notably, the Pareto front is very similar to the one presented in Figure 3, leading to just a 5 % increase in the AVs speed and to invariate fleet sizes. Clearly, the assumption a cost-free automation favours the deployment of AVs at the expenses of subway improvements.
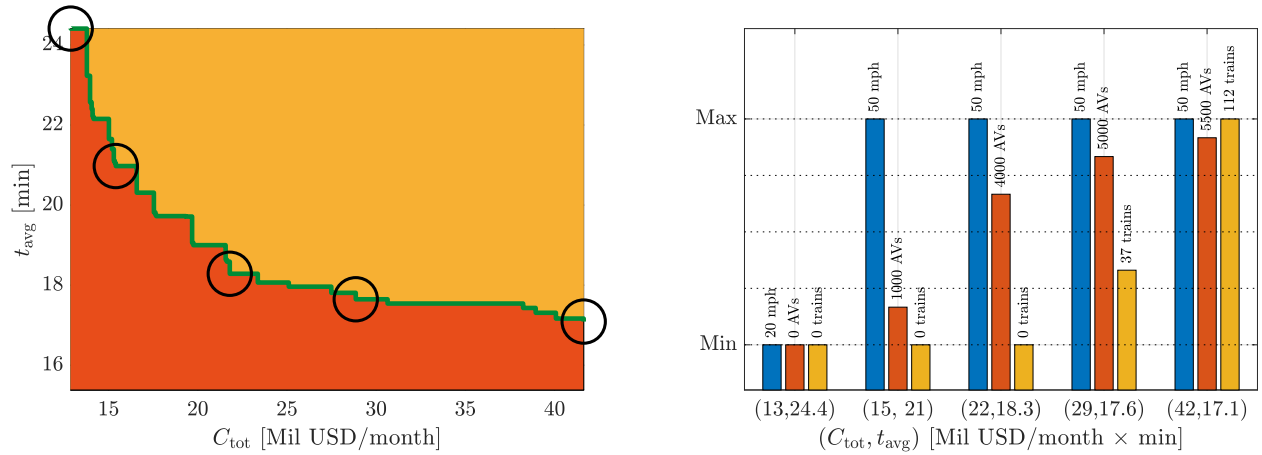
(a) Results for no automation costs.
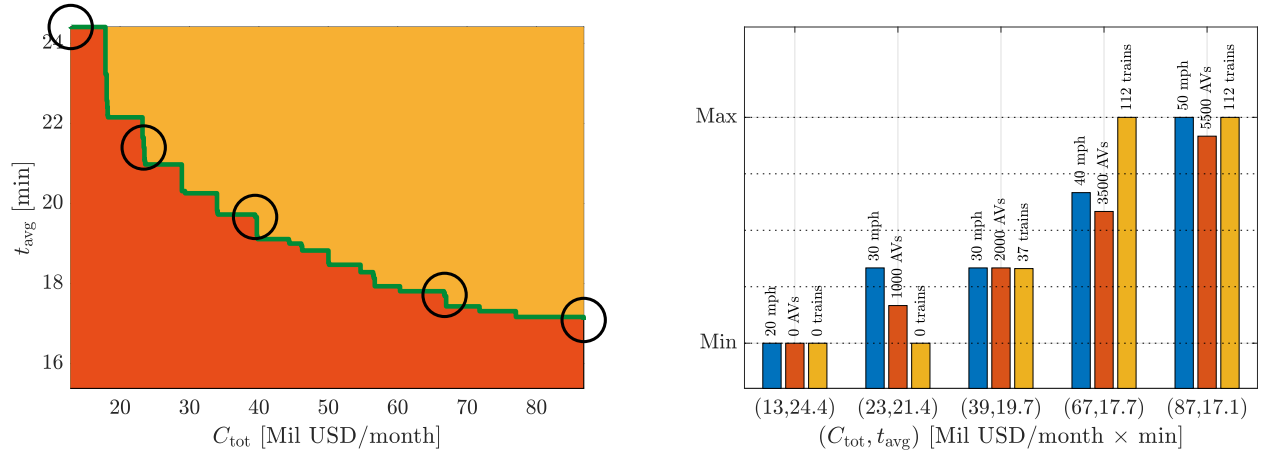
(b) Results for large automation costs.

FIGURE 5: Results for asymptotic automation costs. On the left, the two-dimensional representation of the antichain elements: in red are the unfeasible strategies, in orange the feasible but irrational solutions, and in green the Pareto front. On the right, the implementations corresponding to the highlighted antichain elements.

5.4.2. Case 3.2- High Automation Cost

In this case we assume a performance-independent automation cost of 500,000 USD/car. Although this cost may appear unreasonably large, it roughly captures the extremely onerous research and development costs which AVs companies are facing today [*51*]. Indeed, no company has shown the ability to safely and reliably deploy large fleets of AVs yet. The results, reported in Figure 5b, show different trends from the ones depicted in Figure 5a. First, we observe substantial shift towards an increase of 163 % in the average train fleet size, followed by a 17 % decrease in the average AVs fleet size. Second, to reach the minimal rational average travel time, one needs an expense of roughly 87,000,000 USD/month, corresponding to a 107 % higher investment.

5.5. Discussion

A few comments are in order. First, the presented case studies illustrate the ability of our framework to extract the set of rational design strategies for an AVs-enabled mobility system. This way, stakeholders such as AVs companies, transportation authorities, and policy makers get transparent and interpretable insights on the impact of future interventions. Second, we perform a sensitivity analysis (Figure 6) through the variation of the autonomy cost structures. On the one hand, this reveals a clear transition from small fleets of fast AVs (in the case of low autonomy costs) to a fleet of numerous slow vehicles (in the case of high autonomy costs). On the other hand, our studies highlight that investments in the public transit infrastructure are rational only when large budgets are available. Indeed, the onerous train acquisition and operation costs lead to a comparative advantage of AVs-based mobility. In the future, we plan to collect more high-resolution data to corroborate our conclusions with quantitative results.
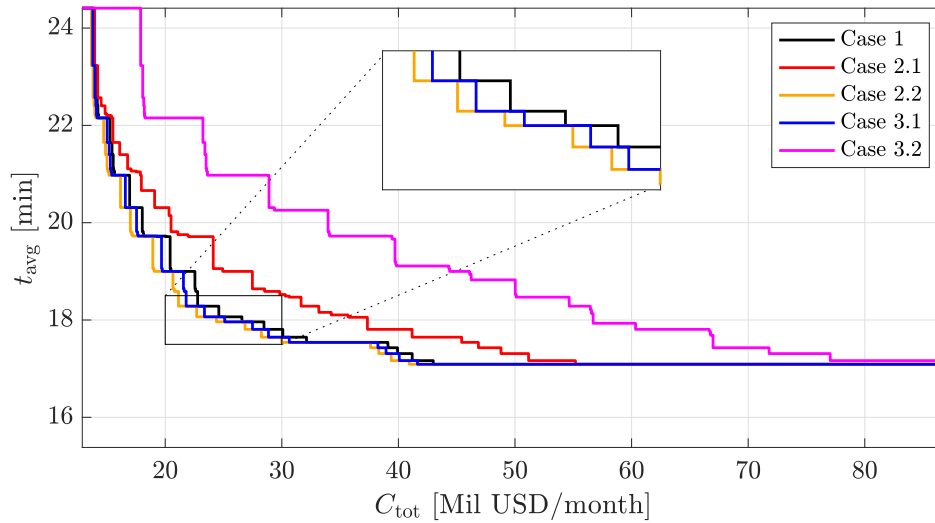

FIGURE 6: Comparison of the antichains resulting from different case studies.

6. Conclusion

In this paper, we leveraged the mathematical theory of co-design to propose a design framework for AVs-enabled mobility systems. Specifically, the nature of our framework allows both for the modular and compositional interconnection of the design problems of different mobility options

and for multiple objectives. Starting from the multi-commodity flow model of an intermodal autonomous mobility-on-demand system, we designed autonomous vehicles and public transit both from a vehicle-centric and fleet-level perspective. In particular, we studied the problem of deploying a fleet of self-driving vehicles providing on-demand mobility in cooperation with public transit, adapting the speed achievable by the vehicles, the fleet size, and the service frequency of the subway lines. Our framework allows the stakeholders involved in the mobility ecosystem, from vehicle developers all the way to mobility-as-a-service companies and governmental authorities, to characterize rational trajectories for technology and investment development. We showcased our methodology on the real-world case study of Washington D.C., USA. Notably, we showed how our problem formulation allows for a systematic analysis of incomparable objectives, providing stakeholders with analytical insights for the socio-technical design of AVs-enabled mobility systems. This work opens the field for the following future research streams:

Modeling: First, we would like to extend the presented framework to capture additional modes of transportation, such as buses, bikes, and e-scooters, and heterogeneous fleets with different self-driving infrastructures, propulsion systems, and passenger capacity. Second, we would like to include the possibility of accommodating the design of public transit lines. Third, we would like to investigate variable demand models. Finally, we would like to analyze the interactions between multiple stakeholders, characterizing the equilibrium arising from their conflicting interests.

Algorithms: It is of interest to tailor general co-design algorithmic frameworks to the particular case of transportation design problems, possibly leveraging their specific structure.

Application: Finally, we would like to devise a web interface which supports mobility stakeholders to reason on strategic interventions in urban areas.

7. Acknowledgements

8. Statement of Contributions
The authors confirm contribution to the paper as follows: study conception and design: Gioele Zardini, Nicolas Lanzetti, Mauro Salazar, Andrea Censi, and Marco Pavone, data collection: Gioele Zardini, Nicolas Lanzetti, analysis and interpretation of results: Gioele Zardini, Nicolas Lanzetti, Mauro Salazar, Andrea Censi, and Marco Pavone, draft manuscript preparation: Gioele Zardini, Nicolas Lanzetti, Mauro Salazar, Andrea Censi, Emilio Frazzoli, and Marco Pavone.
All authors reviewed the results and approved the final version of the manuscript.

9. References

[1] Censi, A., A Mathematical Theory of Co-Design. *arXiv preprint arXiv:1512.08055v7*, 2015.

[2] Censi, A., Monotone Co-Design Problems; or, everything is the same. In *American Control Conference*, 2016.

[3] Censi, A., A Class of Co-Design Problems With Cyclic Constraints and Their Solution. *IEEE Robotics and Automation Letters*, Vol. 2, 2017, pp. 96–103.

[4] Salazar, M., N. Lanzetti, F. Rossi, M. Schiffer, and M. Pavone, Intermodal Autonomous Mobility-on-Demand. *IEEE Transactions on Intelligent Transportation Systems*, 2019, in press.

[5] Farahani, R. Z., E. Miandoabchi, W. Y. Szeto, and H. Rashidi, A review of urban transportation network design problems. *European Journal of Operational Research*, Vol. 229, 2013, pp. 281–302.

[6] Wang, D. Z. W. and H. K. Lo, Global Optimum of the Linearized Network Design Problem with Equilibrium Flows. *Transportation Research Part B: Methodological*, Vol. 44, No. 4, 2010, pp. 482–492.

[7] Cong, Z., B. De Schutter, and R. Babuska, Co-design of traffic network topology and control measures. *Transportation Research Part C: Emerging Technologies*, Vol. 54, 2015, pp. 56–73.

[8] Guihaire, V. and J.-K. Hao, Transit network design and scheduling: A global review. *Transportation Research Part B: Methodological*, Vol. 42, 2008, pp. 1251–1273.

[9] Cipriani, E., S. Gori, and M. Petrelli, Transit network design: a procedure and an application to a large urban area. *Transportation Research Part C: Emerging Technologies*, Vol. 20, No. 1, 2012, pp. 2–14.

[10] Miandoabchi, E., R. Z. Farahani, and W. Y. Szeto, Bi-objective bimodal urban road network design using hybrid metaheuristics. *Central European Journal of Operational Research*, Vol. 20, No. 4, 2012, pp. 583–621.

[11] Barrios, J. A. and J. C. Doig, Fleet sizing for flexible carsharing systems: a simulation-based approach. In *Annual Meeting of the Transportation Research Board*, 2013.

[12] Barrios, J. A. and J. D. Godier, Fleet Sizing for Flexible Carsharing Systems: Simulation-Based Approach. *Transportation Research Record: Journal of the Transportation Research Board*, Vol. 2416, 2014, pp. 1–9.

[13] Fagnant, D. J. and K. M. Kockelman, Dynamic ride-sharing and fleet sizing for a system of shared autonomous vehicles in Austin, Texas. *Transportation*, Vol. 45, No. 1, 2018, pp. 143–158.

[14] Spieser, K., K. Treleaven, R. Zhang, E. Frazzoli, D. Morton, and M. Pavone, Toward a Systematic Approach to the Design and Evaluation of Autonomous Mobility-on-Demand Systems: A Case Study in Singapore. In *Road Vehicle Automation*, Springer, 2014.

[15] Zhang, H., C. J. R. Sheppard, T. Lipman, and M. S. J., Joint Fleet Sizing and Charging System Planning for Autonomous Electric Vehicles. *arXiv preprint arXiv:1811.00234*, 2018.

[16] Beaujon, G. J. and M. A. Turnquist, A Model for Fleet Sizing and Vehicle Allocation. *Transportation Science*, Vol. 25, No. 1, 1991, pp. 19–45.

[17] Liu, Y., P. Bansal, R. Daziano, and S. Samaranayake, A framework to integrate mode choice in the design of mobility-on-demand systems. *Transportation Research Part C: Emerging Technologies*, 2018, in press. Available online at `https://doi.org/10.1016/j.trc.2018.09.022`.

[18] Sayarshad, H. R. and R. Tavakkoli-Moghaddam, Solving a multi periodic stochastic model of the railcar fleet sizing bytwo-stage optimization formulation. Vol. 34, 2010, pp. 1164–1174.

[19] Pinto, H. K. R. F., M. F. Hyland, H. S. Mahmassani, and I. O. Verbas, Joint design of multi-modal transit networks and shared autonomous mobility fleets. *Transportation Research Part C: Emerging Technologies*, 2019, in press. Available online at `https://doi.org/10.1016/j.trc.2019.06.010`.

[20] Davey, B. A. and H. A. Priestley, *Introduction to Lattices and Order*. Cambridge University Press, second edition ed., 2002.

[21] Dahl, D., *If youre annoyed at drivers going under the speed limit, the problem isnt them, its you*. The Bellingham Herald, 2018, available online.

[22] Daganzo, C. F. and N. Geroliminis, An analytical approximation for the macroscopic fundamental diagram of urban traffic. *Transportation Research Part B: Methodological*, Vol. 42, No. 9, 2008, pp. 771–781.

[23] PIM, *Metrorail Ridership by Origin and Destination*. Plan It Metrot, 2012, available online at `https://planitmetro.com/2012/10/31/data-download-metrorail-ridership-by-origin-and-destination/`.

[24] Salazar, M., F. Rossi, M. Schiffer, C. H. Onder, and M. Pavone, On the Interaction between Autonomous Mobility-on-Demand and the Public Transportation Systems. In *Proc. IEEE Int. Conf. on Intelligent Transportation Systems*, 2018, Extended Version, Available at `https://arxiv.org/abs/1804.11278`.

[25] Mas-Colell, A., M. D. Whinston, and J. R. Green, *Microeconomic Theory*. Oxford Univ. Press, 1995.

[26] Richards, D. C., *Relationship between Speed and Risk of Fatal Injury: Pedestrians and Car Occupants*. Department for Transport: London, 2010.

[27] Horni, A., K. Nagel, and K. W. Axhausen (eds.) *The Multi-Agent Transport Simulation MAT-Sim*. Ubiquity Press, 2016.

[28] Haklay, M. and P. Weber, OpenStreetMap: User-Generated Street Maps. *IEEE Pervasive Computing*, Vol. 7, No. 4, 2008, pp. 12–18.

[29] GTFS, *GTFS: Making Public Transit Data Universally Accessible*, 2019, available online at `https://gtfs.org/`.

[30] ODDC, *Taxicab Trips in 2016*. Open Data DC, 2017, available online at `https://opendata.dc.gov/search?q=taxicabs`.

[31] Siddiqui, F., *As ride hailing booms in D.C., it's not just eating in the taxi market – it's increasing vehicle trips*. The Washington Post, 2018, available online.

[32] DoA (ed.) *Military Police Traffic Operations*. Department of the Army, 1977.

[33] Dixon, S., H. Irshad, and V. White, *Deloitte City Moblity Index – Washington D.C.* Deloitte, 2018.

[34] Censi, A., *Monotone Co-Design Problems*, 2019, available online: `https://co-design.science/index.html`.

[35] Pavlenko, N., P. Slowik, and N. Lutsey, *When does electrifying shared mobility make economic sense?* The International Council on Clean Transportation, 2019.

[36] Boesch, P. M., F. Becker, H. Becker, and K. W. Axhausen, Cost-based analysis of autonomous mobility services. *Transport Policy*, Vol. 64, 2018, pp. 76–91.

[37] Fagnant, D. J. and K. Kockelman, Preparing a nation for autonomous vehicles: opportunities, barriers and policy recommendations. *Transportation Research Part A: Policy and Practice*, Vol. 77, 2015, pp. 167–181.

[38] Bauer, G. S., J. B. Greenblatt, and B. F. Gerke, Cost, Energy, and Environmental Impact of Automated Electric Taxi Fleets in Manhattan. *Environmental Science & Technology*, Vol. 52, No. 8, 2018, pp. 4920–4928.

[39] Litman, T., *Autonomous Vehicle Implementation Predictions – Implications for Transport Planning*. Victoria Transport Policy Institute, 2019.

[40] Wadud, Z., Fully automated vehicles: A cost of ownership analysis to inform early adoption. *Transportation Research Part A: Policy and Practice*, Vol. 101, 2017, pp. 163–176.

[41] Time, W., *Carboon Footprint Data*, 2018, Available at `https://api.watttime.org`. Retrieved on March 23, 2018.

[42] WMATA, *FY2018 Proposed Budget*. Washington Metropolitan Area Transit Authority, 2017.

[43] Aratani, L., *Metro to debut first of its 7000-series cars on Blue Line on April 14*. The Washington Post, 2015, available online.

[44] WMATA, *Sustainability Report 2018*. Washington Metropolitan Area Transit Authority, 2018.

[45] Jaffe, E., *The Case for Driverless Trains, By the Numbers*. Citylab, 2015, available online.

[46] Howard, P. and D. Sylvan, *Expert Consensus on the Economics of Climate Change*. Institute for Policy Integrity – New York University School of Law, 2015.

[47] Wang, Y., J. Zhang, M. Ma, and X. Zhoum, Survey on Driverless Train Operation for Urban Rail Transit Systems. Vol. 2, No. 3–4, 2016, pp. 106–113.

[48] Gawron, J. H., G. A. Keoleian, R. D. De Kleine, T. J. Wallington, and K. Hyung Chul, Life Cycle Assessment of Connected and Automated Vehicles: Sensing and Computing Subsystem and Vehicle Level Effects. *Environmental Science & Technology*, Vol. 52, 2018, pp. 3249–3256.

[49] WCP, *The Automotive LiDAR Market*. Woodside Capital Partners, 2018.

[50] Lienert, P., *Cost of Driverless Vehicles to Drop Dramatically: Delphi CEO*. Insurance Journal, 2019, available online.

[51] Korosec, K., *Uber spent USD 457 million on self-driving and flying car R&D last year*. TechCrunch, 2019, available online.